# Green's-function calculation of electron screening in a plasma

M. J. Watrous, L. Wilets, and J. J. Rehr
*Department of Physics, Box 351560, University of Washington, Seattle, Washington 98195-1560*
(Received 13 April 1998)

Extensions to the finite temperature Green's-function method for the calculation of equilibrium densities within the Kohn-Sham formulation of density functional theory are presented. In particular, an expression for the density in terms of single-particle Green's-function differences summed over all Matsubara poles is utilized. Numerical methods for the evaluation of this infinite sum are given. This formulation automatically includes discrete as well as continuum states, is valid for finite temperatures, and is especially well suited for high temperatures. Techniques are also presented for the calculation of single-particle Green's functions for spherically symmetric systems and arbitrary complex energies. The usefulness of these methods is demonstrated by their application to the problem of electron screening of nuclei in a plasma. Direct comparison is made with previous finite temperature, Kohn-Sham, wave function type calculations for protons and for neon nuclei in an electron gas. [S1063-651X(99)07203-7]

PACS number(s): 52.20.Hv, 31.10.+z, 31.15.Ew

## I. INTRODUCTION

The Kohn-Sham formulation [1] of density functional theory [2,3] is the modern day descendent of the Hartree approximation [4]. The common goal of these approaches is to represent a solution to the many-body problem in terms of single-particle wave functions which are acted upon by an effective potential. These wave functions are typically calculated as eigenfunctions of single-particle Schrödinger equations, and their squares are summed to yield the density for the system.

An alternative prescription for the evaluation of the density makes use of single-particle Green's functions [5]. By definition these Green's functions sum over all of the eigenfunctions for the system, both discrete and continuum. They are expressed in terms of their spectral representation and are calculated as the solutions of their defining differential equations. In this method, the density is given by an integral of the Green's function along an appropriate contour in the complex energy plane. It should be noted that the calculation of the Green's functions involves one-sided boundary value problems only and does not require the determination of eigenvalues or phase shifts.

A variation of the Green's-function method for finite temperatures has been developed by Dederichs, Zeller, and their collaborators [6–8]. Their approach is limited to relatively low temperatures, however, due to its dependence on the Sommerfeld expansion [9] for the Fermi occupation factor. For the higher temperatures found in many astrophysical and terrestrial systems, a different implementation of the Green's-function method is required. This is the subject of the present work.

In order to extend the method to higher temperatures, an alternative contour in the complex energy plane is chosen such that the density is given by a sum of differences in Green's functions evaluated at all of the Matsubara poles. This contour has been considered previously [6], but it was not pursued due to two obstacles: the infinite number of poles for which Green's functions must be calculated and the increasing difficulty in calculating the Green's functions for ever larger values of the complex energy.

Both of these difficulties are surmounted here. First, the number of Green's functions that are required is limited by extrapolation and interpolation. An asymptotic expression has been derived, which is employed to approximate the sum of Green's-function differences beyond the last Matsubara pole for which they are calculated. Second, an approach for the evaluation of the high-lying Matsubara poles has been developed. For large values of the complex energy, the differential equations are simplified from second to first order by writing the Green's functions in terms of logarithmic derivatives. These derivatives become increasingly smooth as the complex energy increases.

To demonstrate the method's utility, the electron densities surrounding protons and neon nuclei embedded in an electron gas have been calculated for various temperatures and electron densities. To demonstrate the method's advantages, the results are compared with previous Kohn-Sham, wave function calculations.

## II. DENSITIES VIA CONTOUR INTEGRATION OF GREEN'S FUNCTIONS

### A. The electron density

Making use of the finite temperature generalization of density functional theory due to Mermin [10], the equilibrium density $\rho(\vec{r})$ of an interacting, many-electron system, acted upon by an external potential $v(\vec{r})$, is expressed as

$$\rho(\vec{r}) = \sum_i |\phi_i(\vec{r})|^2 f(\epsilon_i), \tag{1}$$

where the single-particle wave functions satisfy

$$\left[ -\frac{1}{2}\nabla^2 + v_{\rm eff}(\vec{r}) \right] \phi_i(\vec{r}) = \epsilon_i \phi_i(\vec{r}), \tag{2}$$

and the effective potential is given by

 

$$v_{\rm eff}(\vec{r}) = v(\vec{r}) + \int d^3r' \frac{\rho(\vec{r}')}{|\vec{r}-\vec{r}'|} + v_{\rm xc}[\rho(\vec{r})]. \quad (3)$$

The Fermi occupation factor,

$$f(\epsilon) = \frac{1}{e^{(\epsilon-\mu)/T}+1}, \quad (4)$$

depends on the temperature $T$ and chemical potential $\mu$ of the electrons. The self-consistent solution of these equations yields the equilibrium density. The sum in the expression for the electron density is over the complete set of energy eigenvalues, bound and free. Depending on the temperature and density, bound states may or may not exist. Note that throughout this work atomic units are used ($m_e = e = \hbar = k_B = 1$).

In the above expression, the exchange-correlation potential $v_{\rm xc}$ is the temperature dependent functional derivative of the exchange and correlation contributions to the grand potential. For simplicity, the discussion here is limited to spin symmetric systems and spin independent exchange-correlation potentials.

### B. A nucleus in an electron gas

The following model is considered for the shielding of a nucleus with atomic number $Z$ in a neutral plasma. The nucleus is taken to be embedded in a positive jellium and surrounded by an electron gas with average density $\rho_0$. The jellium models the remaining nuclei in the plasma and has charge density equal to the average electron density.

The external potential $v(\vec{r})$ which acts upon the electrons is due to the nucleus and the jellium. The effective potential for this problem is thus

$$\bar{v}_{\rm eff}(\vec{r}) = -\frac{Z}{r} + \int \frac{\rho(\vec{r}')-\rho_0}{|\vec{r}-\vec{r}'|} d^3r' + v_{\rm xc}[\rho(\vec{r})] - v^0_{\rm xc}. \quad (5)$$

At distances far from the nucleus, the effective potential approaches that of a uniform electron gas $v_{\rm xc0} = v_{\rm xc}[\rho_0]$. The bar over the effective potential indicates that this residual exchange-correlation potential has been removed and that the barred effective potential vanishes outside the range of the nucleus. The same subtraction is also applied to the eigenvalues of the single-particle Schrödinger equations $\bar{\epsilon}$ and to the chemical potential of the electrons $\bar{\mu}$.

The average density and the temperature fix the barred chemical potential in the usual way,

$$\rho_0(T,\bar{\mu}) = \frac{N}{V} = 2\int \frac{d^3p}{(2\pi)^3} \frac{1}{e^{(p^2/2-\bar{\mu})/T}+1}, \quad (6)$$

where $N$ is the number of electrons in a uniform electron gas of volume $V$, including a factor of 2 due to spin degeneracy.

### C. The Green's functions

The single-particle Green's function associated with the effective potential $\bar{v}_{\rm eff}$ can be written in terms of its spectral representation as

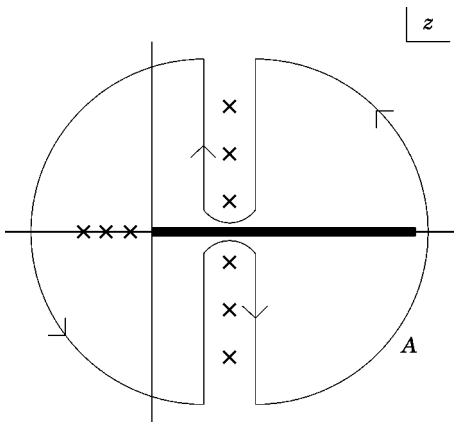


FIG. 1. Contour enclosing the poles in $\mathcal{G}(\vec{r},\vec{r}';z)$ at all of the energy eigenvalues for a nucleus in a finite temperature plasma. The cut along the real axis of course extends to $+\infty$ but does not contribute for large $x$ in the difference $G-G^{(0)}$ which vanishes as $|z| \to \infty$.

$$G(\vec{r},\vec{r}';z) = \sum_i \frac{\phi_i(\vec{r})\phi_i^*(\vec{r}')}{z-\bar{\epsilon}_i}. \quad (7)$$

Due to the completeness of the wave functions the Green's function satisfies

$$\left[-\frac{1}{2}\nabla^2 + \bar{v}_{\rm eff}(\vec{r}) - z\right] G(\vec{r},\vec{r}';z) = -\delta^3(\vec{r}-\vec{r}'). \quad (8)$$

For convenience, the product of the Green's function and the Fermi factor, which is written explicitly as a function of energy and chemical potential, is defined as

$$\mathcal{G}(\vec{r},\vec{r}';z) = G(\vec{r},\vec{r}';z) f(z,\bar{\mu}). \quad (9)$$

The analytic structure of this function is shown in Fig. 1. It has poles at the energy eigenvalues with residues $\phi_i(\vec{r})\phi_i^*(\vec{r}') f(\bar{\epsilon}_i,\bar{\mu})$. It also has poles at the Matsubara frequencies,

$$z_j = \bar{\mu} \pm i\pi(2|j|-1)T, \quad j = \pm 1, \pm 2, \pm 3, \ldots \quad (10)$$

with residues $-TG(\vec{r},\vec{r}';z_j)$.

The contour $A$ in Fig. 1 encloses the poles at all of the energy eigenvalues along the real axis, bound and free. As shown in Fig. 2, this contour can be deformed into the set of contours $B_j$, each of which encloses a Matsubara pole, plus the contour $C$ at infinity. The integrals along these contours are related as follows:

$$\oint_A \mathcal{G}(\vec{r},\vec{r}';z)dz = -\sum_j \oint_{B_j} \mathcal{G}(\vec{r},\vec{r}';z)dz + \oint_C \mathcal{G}(\vec{r},\vec{r}';z)dz, \quad (11)$$

where the minus sign is a result of the direction of integration around the Matsubara poles. The residue theorem can be applied to yield

$$\rho(\vec{r}) = T\sum_j G(\vec{r},\vec{r};z_j) + \frac{1}{\pi i}\oint_C \mathcal{G}(\vec{r},\vec{r};z)dz. \quad (12)$$

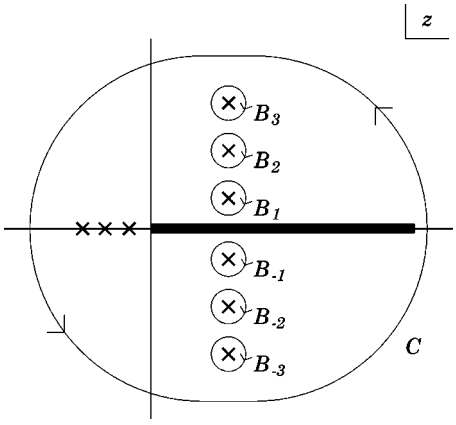


FIG. 2. A set of contours equivalent to that of the previous figure which encloses all of the Matsubara poles and which has a contour at infinity.

This expression includes a factor of 2 due to the spin symmetry of a finite temperature plasma, where all spin states are occupied to some degree.

Note that the integrand does not vanish along the contour $C$, and the Green's functions for a uniform system are therefore required to cancel this integral.

The uniform system in this case is simply a constant electron gas of density $\rho_0$ plus the jellium background. As a result, its effective potential $\overline{v}_{\rm eff}^{(0)}(\vec{r})$ is zero. For this uniform system, a Green's function $G^{(0)}(\vec{r},\vec{r}';z)$ can be defined in analogy to Eq. (7), and a function $\mathcal{G}^{(0)}(\vec{r},\vec{r}';z)$ can similarly be defined corresponding to Eq. (9). The density of the uniform system can then be expressed in the form of Eq. (12).

### D. The induced density via Green's-function differences

For large values of the complex energy $z$, the Green's functions $G$ and $G^{(0)}$ are equal, and the integrals over the contour $C$ are thus also equal. That the difference of the two Green's functions vanishes for large complex energies is shown in a later section of this paper.

If the induced density is defined as

$$\Delta\rho(\vec{r})=\rho(\vec{r})-\rho^{(0)}(\vec{r}), \tag{13}$$

then it is given by the following sum over Green's-function differences:

$$\Delta\rho(\vec{r})=4T\sum_{j=1}^{\infty}\ {\rm Re}[G(\vec{r},\vec{r};z_j)-G^{(0)}(\vec{r},\vec{r};z_j)]. \tag{14}$$

This result has been simplified using the relation $G(\vec{r},\vec{r};z^*)=G^*(\vec{r},\vec{r};z)$, and it is restricted to spin degenerate exchange-correlation potentials.

This expression for the density requires the Green's-function differences for values of the complex energy ranging from small to arbitrarily large. For systems such as a single nucleus in a plasma, the Green's functions are spherically symmetric. Techniques are presented in the next section which make possible the calculation of these Green's functions for all values of the complex energy.

## III. GREEN'S FUNCTIONS FOR SPHERICALLY SYMMETRIC SYSTEMS

### A. The radial Green's functions

The Green's function for a spherically symmetric system can be written as

$$G(\vec{r},\vec{r}';z)=\frac{1}{2\pi rr'}\sum_{l=0}^{\infty}(2l+1)g_l(r,r';z)P_l(\cos\gamma). \tag{15}$$

For a given complex energy, a new notation is introduced for the radial Green's function,

$$g_{l,\kappa}(r,r')=g_l(r,r';z=\kappa^2/2), \tag{16}$$

where the complex wave number is defined as $\kappa=\sqrt{-2z}$, ${\rm Re}[\kappa]>0$. The radial Green's functions are taken to be

$$g_{l,\kappa}(r,r')=\frac{\psi_{l,\kappa}(r_<)\chi_{l,\kappa}(r_>)}{W[\psi_{l,\kappa},\chi_{l,\kappa}]}. \tag{17}$$

Here, $P_l$ is the Legendre polynomial of order $l$, and $\gamma$ is the angle between $\vec{r}$ and $\vec{r}'$. The functions $\psi_{l,\kappa}$ and $\chi_{l,\kappa}$ are solutions of the radial differential equations

$$\left[-\frac{d^2}{dr^2}+\frac{l(l+1)}{r^2}+2\overline{v}_{\rm eff}(r)+\kappa^2\right]\begin{Bmatrix}\psi_{l,\kappa}(r)\\ \chi_{l,\kappa}(r)\end{Bmatrix}=0, \tag{18}$$

which are regular at the origin and at large $r$, respectively. Since the above differential equation has no first-order derivative, the Wronskian of its solutions,

$$W[\psi_{l,\kappa},\chi_{l,\kappa}]=\psi_{l,\kappa}(r)\chi'_{l,\kappa}(r)-\psi'_{l,\kappa}(r)\chi_{l,\kappa}(r), \tag{19}$$

is independent of $r$. The radial Green's function satisfies the inhomogeneous differential equation,

$$\left[-\frac{d^2}{dr^2}+\frac{l(l+1)}{r^2}+2\overline{v}_{\rm eff}(r)+\kappa^2\right]g_{l,\kappa}(r,r')=-\delta(r-r'). \tag{20}$$

### B. The radial Green's functions in terms of known functions

Depending on their complex energy, the radial Green's functions are calculated using two different methods. The first approach makes use of known functions to remove the dominant behaviors from the solutions of the radial equations, $\psi_{l,\kappa}$ and $\chi_{l,\kappa}$.

Near the origin, the differential equations for the radial solutions are dominated by the Coulomb potential of the nucleus and by the centrifugal potential. Therefore, the product forms of the solutions in this region are taken to be

$$\psi_{l,\kappa}(r)=F_l(\eta,p)\overline{\psi_{l,\kappa}}(r), \tag{21}$$

$$\chi_{l,\kappa}(r)=H_l^{(+)}(\eta,p)\overline{\chi_{l,\kappa}}(r), \tag{22}$$

where $F_l$ and $H_l^{(+)}$ are Coulomb wave functions of the first and third kind [11,12], which are regular at the origin and at large $r$, respectively, where $\eta=iZ/\kappa$, and where $p=i\kappa r$.

Far from the origin, the screening of the electrons causes the effective potential to vanish. As a result, the radial solutions there should be similar in form to those of a system with no central nucleus. The product forms of the solutions in this region are thus taken to be

$$\psi_{l,\kappa}(r)=\psi^{(0)}_{l,\kappa}(r)\overline{\psi_{l,\kappa}}(r), \tag{23}$$

$$\chi_{l,\kappa}(r)=\chi^{(0)}_{l,\kappa}(r)\overline{\chi_{l,\kappa}}(r), \tag{24}$$

where $\psi^{(0)}_{l,\kappa}$ and $\chi^{(0)}_{l,\kappa}$ are the radial solutions for the uniform system. The uniform radial solutions satisfy Eq. (18) when its effective potential is set to zero, and they are related to the spherical Bessel functions of the first and third kind [11,13] by

$$\psi^{(0)}_{l,\kappa}(r)=rj_l(i\kappa r), \tag{25}$$

$$\chi^{(0)}_{l,\kappa}(r)=rh^{(1)}_l(i\kappa r). \tag{26}$$

For both regions, the barred functions are calculated by numerical integration of the differential equations which follow from the substitution of the above product forms into Eq. (18). The Coulomb wave functions and spherical Bessel functions, on the other hand, are evaluated using computer routines [11,14] available from the CERN program library [15].

### C. The radial Green's functions in terms of logarithmic derivatives

As the complex energy values in Eq. (29) increase, the methods of the preceding section become increasingly more difficult to evaluate, and a second method for numerically calculating the radial Green's functions is needed. A new approach is introduced here which makes use of logarithmic derivatives and which becomes more efficient as $z$ increases.

This approach makes use of the following relationship between the logarithmic derivatives of the radial solutions, $\psi_{l,\kappa}$ and $\chi_{l,\kappa}$:

$$\left(\frac{\chi'_{l,\kappa}(r)}{\chi_{l,\kappa}(r)}\right)-\left(\frac{\psi'_{l,\kappa}(r)}{\psi_{l,\kappa}(r)}\right)=\frac{W[\psi_{l,\kappa},\chi_{l,\kappa}]}{\psi_{l,\kappa}(r)\chi_{l,\kappa}(r)}. \tag{27}$$

This expression follows from the definition of the Wronskian, Eq. (19), and its right hand side is just the reciprocal of the radial Green's function evaluated for $r=r'$. The Green's function can therefore be calculated in terms of differences of logarithmic derivatives,

$$g_{l,\kappa}(r,r)=\left[\left(\frac{\chi'_{l,\kappa}(r)}{\chi_{l,\kappa}(r)}\right)-\left(\frac{\psi'_{l,\kappa}(r)}{\psi_{l,\kappa}(r)}\right)\right]^{-1}. \tag{28}$$

Both logarithmic derivatives can be shown to satisfy the nonlinear, first-order differential equation

$$\frac{d}{dr}\left(\frac{\psi'_{l,\kappa}(r)}{\psi_{l,\kappa}(r)}\right)=\left[\frac{l(l+1)}{r^2}+2\overline{v}_{\rm eff}(r)+\kappa^2\right]-\left(\frac{\psi'_{l,\kappa}(r)}{\psi_{l,\kappa}(r)}\right)^2. \tag{29}$$

This transformation of a differential equation from second to first order by means of the logarithmic derivative of its solutions is due to Riccati [16]. At the origin and at large $r$ they behave as

$$\left(\frac{\psi'_{l,\kappa}(r)}{\psi_{l,\kappa}(r)}\right)\rightarrow\begin{cases}(l+1)/r & \text{for } r\rightarrow 0\\ +\kappa & \text{for } |\kappa r|\rightarrow\infty,\end{cases} \tag{30}$$

$$\left(\frac{\chi'_{l,\kappa}(r)}{\chi_{l,\kappa}(r)}\right)\rightarrow\begin{cases}-l/r & \text{for } r\rightarrow 0\\ -\kappa & \text{for } |\kappa r|\rightarrow\infty.\end{cases} \tag{31}$$

Whereas the asymptotic forms of the radial solutions become more and more oscillatory as the complex energy increases, the logarithmic derivatives are more slowly varying in this limit, approaching values of $\pm\kappa$.

The work required for the calculation of the logarithmic derivatives is simplified in the same manner as is used for small values of the complex energy. That is, the radial grid is divided into two regions, and the leading order behaviors of the logarithmic derivatives in each region are extracted. This leaves well behaved functions to be calculated numerically.

## IV. EVALUATION OF THE DENSITY

### A. The spherically symmetric density

For spherically symmetric systems, the density is expanded in terms of contributions from the angular momentum components of the Green's functions,

$$\Delta\rho(r)=\frac{1}{r^2}\sum_{l=0}^{\infty}\Delta\rho_l(r). \tag{32}$$

Substitution of the spherically symmetric Green's function, Eq. (15), into the density expression, Eq. (14), shows that the induced density components are

$$\Delta\rho_l(r)=\frac{2(2l+1)}{\pi}T\sum_{j=1}^{\infty}\mathrm{Re}[\Delta g_{l,\kappa_j}(r,r)], \tag{33}$$

where

$$\Delta g_{l,\kappa}(r,r')=g_{l,\kappa}(r,r')-g^{(0)}_{l,\kappa}(r,r'). \tag{34}$$

As written, the induced density involves a sum of Green's-function differences evaluated for an infinite number of Matsubara poles. In practice, the number of Green's functions that can be calculated is finite, and extrapolation and interpolation are used to evaluate the complete sum.

Let $M$ be the index of the largest pole $z_M$ for which the Green's functions are calculated. The sum of the Green's functions for poles beyond this maximum pole $z_M$ is approximated by extrapolation of an asymptotic expression for the Green's-function differences. This expression is derived below.

### B. An asymptotic expression for the radial Green's functions

The centrifugal and effective potentials in Eq. (20) are combined to form a total potential

$$V_l(r) = \frac{l(l+1)}{r^2} + 2\overline{v}_{\rm eff}(r). \tag{35}$$

Let $\tilde{g}_\kappa$ be the solution of Eq. (20) for the case where the total potential $V_l$ is zero. This Green's function has the well known form [17]

$$\tilde{g}_\kappa(r,r') = -\frac{e^{-\kappa|r-r'|}}{2\kappa}. \tag{36}$$

The Born series [18] for the radial Green's function $g_{l,\kappa}$ in terms of $\tilde{g}_\kappa$ can be written symbolically as

$$g_{l,\kappa} = \tilde{g}_\kappa + \int \tilde{g}_\kappa V_l \tilde{g}_\kappa + \int\int \tilde{g}_\kappa V_l \tilde{g}_\kappa V_l \tilde{g}_\kappa + \cdots. \tag{37}$$

This expression can be evaluated for $r' = r$ to give

$$g_{l,\kappa}(r,r) = -\frac{1}{2\kappa} + \frac{V_l(r)}{4\kappa^3} - \frac{3V_l^2(r) - V_l''(r)}{16\kappa^5} + O\left(\frac{1}{\kappa^7}, \frac{e^{-2\kappa r}}{\kappa^3}\right). \tag{38}$$

For the remainder of this discussion, terms of order $\kappa^{-3}e^{-2\kappa r}$, or less, are neglected.

The first three terms in this expression can be used to approximate the radial Green's function for large values of $\kappa$. Each term in the expression is smaller than the previous by a factor which is essentially of the order of $V_l(r)/\kappa^2$. Thus, the expression is only convergent for those values of $r$ where $\kappa^2$ dominates $V_l(r)$ in the differential equation. In other words, for a given $\kappa$ value, Eq. (38) is a useful representation of the radial Green's function, $g_{l,\kappa}$, only in those regions where the differential equations for $g_{l,\kappa}$ and $\tilde{g}_\kappa$ are nearly the same, and hence where $g_{l,\kappa}$ is accurately given by $\tilde{g}_\kappa$ plus a few correction terms.

### C. A previous expression

It should be noted that Kohn and Sham [19] have also considered the Born series for Green's functions, Eq. (37), for the case of a general one-dimensional potential $V(r)$. Their result for the Green's function differs from Eq. (38) in that it contains an extra term of order $\kappa^{-4}$, which depends on the first derivative of the potential.

The source of the derivatives in Eq. (38) is the Taylor expansion of the potential $V$ about $r$. It can be shown that the term coming from the first derivative gives a contribution to the integrals in Eq. (37) that is of order $\kappa^{-3}e^{-2\kappa r}$. For large $\kappa$ this term is negligible, and the asymptotic expression for the radial Green's function in Eq. (38) is therefore correct.

The validity of Eq. (38) can also be demonstrated by explicit construction of the asymptotic form of the uniform radial Green's function $g^{(0)}_{l,\kappa}(r,r)$ using known forms for the spherical Bessel functions.

### D. Limiting the number of calculated Green's functions

The difference in Green's functions is the quantity of interest in this calculation. Since the asymptotic expression for the uniform radial Green's function $g^{(0)}_{l,\kappa}(r,r)$ is just Eq. (38) evaluated with the total potential $V_l^{(0)}$, the radial Green's-function difference is given by

$$\Delta g_{l,\kappa}(r,r) = \frac{a(r)}{\kappa^3} + \frac{b_l(r)}{\kappa^5} + O\left(\frac{1}{\kappa^7}\right), \tag{39}$$

where

$$a(r) = \frac{1}{2}\overline{v}_{\rm eff}(r), \tag{40}$$

$$b_l(r) = -\frac{3}{4}\left[\overline{v}^2_{\rm eff}(r) + \frac{l(l+1)}{r^2}\overline{v}_{\rm eff}(r)\right] + \frac{1}{8}\overline{v}''_{\rm eff}(r). \tag{41}$$

It should be noted that the leading order term in the Green's-function differences depends on the effective potential $\overline{v}_{\rm eff}$ and not on the total potential $V_l$. Taking the difference of the Green's functions cancels their common centrifugal barriers. This result shows that the difference of the Green's functions goes to zero more rapidly than the Green's functions themselves. It also verifies the conjecture of Sec. II D that the difference of the Green's function vanishes along the contour $C$, where the complex energy $z$, and thus $\kappa$, go to infinity.

The sum of the Green's-function differences beyond the last Matsubara pole for which they are calculated, $z_M$ is extrapolated using Eq. (39) and the value calculated for the Green's-function difference at $z_M$. That is, the sum over Green's-function differences beyond the last calculated pole is approximated by

$$\sum_{j=M+1}^{\infty} {\rm Re}[\Delta g_{l,\kappa_j}(r,r)] \approx \sum_{j=M+1}^{\infty} {\rm Re}\left[\frac{a(r)}{\kappa_j^3} + \frac{b_l(r)}{\kappa_j^5} + \frac{c_l(r;z_M)}{\kappa_j^7}\right], \tag{42}$$

where the coefficient $c_l$ is determined from the Green's-function difference at $z_M$,

$$\Delta g_{l,\kappa_M}(r,r) = \frac{a(r)}{\kappa_M^3} + \frac{b_l(r)}{\kappa_M^5} + \frac{c_l(r;z_M)}{\kappa_M^7}. \tag{43}$$

The sum of the extrapolated Green's-function differences in Eq. (42) is evaluated using the Euler-Maclaurin summation formula [20].

Consider the choice of $z_M$. For particular values of $l$ and $r$, $z_M$ must be large enough that the asymptotic forms in Eq. (39) can be used to extrapolate the Green's-function differences. At lower temperature, the value of $M$ will be much higher, because the separation of the poles is proportional to $T$, Eq. (10). In general, then, the lower the temperature, the more poles that will be needed, and the more Green's functions which must be evaluated.

In order to limit the number of poles for which Green's functions must be calculated, the sum of the $M$ radial Green's-function differences up to $z_M$ is also approximated in this calculation. Specifically, the Green's-function differences are calculated for some of the poles and their values for the remaining poles are determined by interpolation. This is feasible because the radial Green's-function differences are very well behaved as functions of the complex energy $z$. The interpolation scheme that is used most heavily weighs those values of the complex energy $z$ close to the real axis. For larger values of $z$, the Green's-function differences approach their asymptotic forms and thus require fewer calculated values for accurate interpolation.

Further details concerning the evaluation of the density are given elsewhere [21].

### E. Asymptotic expressions for the logarithmic derivatives

The analysis of the asymptotic forms for the logarithmic derivatives of the radial solutions parallels that of the preceding section. In this case, the asymptotic forms are

$$\left(\frac{\psi'_{l,\kappa}(r)}{\psi_{l,\kappa}(r)}\right) = +\kappa + \frac{V_l(r)}{2\kappa} - \frac{V'_l(r)}{4\kappa^2} - \frac{V_l^2(r) - V''_l(r)}{8\kappa^3} + O\left(\frac{1}{\kappa^4}\right) \tag{44}$$

and

$$\left(\frac{\chi'_{l,\kappa}(r)}{\chi_{l,\kappa}(r)}\right) = -\kappa - \frac{V_l(r)}{2\kappa} - \frac{V'_l(r)}{4\kappa^2} + \frac{V_l^2(r) - V''_l(r)}{8\kappa^3} + O\left(\frac{1}{\kappa^4}\right). \tag{45}$$

Note that most of these terms are of opposite sign, except for the first derivatives. As a check, these forms for the logarithmic derivatives can be substituted into the radial Green's function of Eq. (28) to reproduce its asymptotic form, Eq. (38).

These expressions are used to speed the computation of the logarithmic derivatives in those regions where $V_l(r)$ is small compared to $\kappa$.

## V. NUCLEI IN AN ELECTRON GAS

### A. A proton in an electron gas

The Green's-function method of this paper is now applied to the problem of the screening of nuclei in an electron gas. Electron densities calculated using the Green's-function method are compared with densities calculated using Kohn-Sham wave function techniques.

For the case of the screening of a proton, comparison is made with a calculation due to Perrot [22]. The parameters which were considered by Perrot are listed in Table I, and the results from the two methods are shown in Table II. The induced electron density values at the origin are given, along with the inverse screening length implied by the density distribution. The first set of values are the results calculated using the Green's-function method. The second set contains the values due to Perrot.

TABLE I. Parameters used in Perrot's proton calculation. All values are in atomic units, where $\rho_0 = 1.0$ a.u. is equal to 6.75 electrons $\text{Å}^{-3}$ and $T = 1.0$ a.u. is equal to $3.16 \times 10^5$ K. The chemical potential $\bar{\mu}$ is calculated with the residual exchange-correlation potential removed.

| $r_s$ | $t = T/T_F$ | $\rho_0$ | $T$ | $T_F$ | $\bar{\mu}$ |
|---|---|---|---|---|---|
| 1.0 | 0.5 | 0.239 | 0.921 | 1.842 | 1.3685 |
| 1.0 | 1.0 | 0.239 | 1.842 | 1.842 | −0.0395 |
| 1.0 | 2.0 | 0.239 | 3.683 | 1.842 | −4.5329 |
| 2.0 | 0.5 | 0.0298 | 0.230 | 0.460 | 0.34213 |
| 2.0 | 1.0 | 0.0298 | 0.460 | 0.460 | −0.00988 |
| 2.0 | 2.0 | 0.0298 | 0.921 | 0.460 | −1.13323 |
| 4.0 | 0.5 | 0.00373 | 0.0575 | 0.1151 | 0.08553 |
| 4.0 | 1.0 | 0.00373 | 0.1151 | 0.1151 | −0.00247 |
| 4.0 | 2.0 | 0.00373 | 0.2302 | 0.1151 | −0.28331 |

In both cases, the local density approximation is made for the temperature dependent exchange-correlation potential using a parametrization due to Perrot and Dharma-wardana [23]. The correlation contributions to the grand potential in this parametrization are treated via the random phase approximation.

The inverse screening length $k$, not to be confused with the wave vector, is introduced here for the purpose of comparison with Perrot. If the induced density is assumed to be of the form

$$\Delta\rho(r) = \frac{Zk^2}{4\pi r} e^{-kr}, \tag{46}$$

then the total induced charge inside a sphere of radius $R_0 = 2/k$ is

$$\int_0^{R_0} \Delta\rho(r) 4\pi r^2 \, dr = 0.594Z. \tag{47}$$

TABLE II. The induced electron density at the proton $\Delta\rho(0)$ and the inverse screening length $k$ calculated using the Green's-function method, and the same quantities for the standard density functional calculation due to Perrot.

| | | This work | | Perrot | |
|---|---|---|---|---|---|
| $r_s$ | $t$ | $\Delta\rho(0)$ | $k$ | $\Delta\rho(0)$ | $k$ |
| 1.0 | 0.5 | 0.853 | 1.633 | 0.841 | 1.623 |
| 1.0 | 1.0 | 0.695 | 1.285 | 0.682 | 1.276 |
| 1.0 | 2.0 | 0.498 | 0.922 | 0.486 | 0.928 |
| 2.0 | 0.5 | 0.435 | 1.460 | 0.428 | 1.454 |
| 2.0 | 1.0 | 0.357 | 1.134 | 0.349 | 1.114 |
| 2.0 | 2.0 | 0.240 | 0.741 | 0.235 | 0.729 |
| 4.0 | 0.5 | 0.335 | 1.426 | 0.338 | 1.426 |
| 4.0 | 1.0 | 0.309 | 1.275 | 0.306 | 1.266 |
| 4.0 | 2.0 | 0.232 | 0.878 | 0.222 | 0.839 |

TABLE III. Parameters for which Friedel oscillations were found. The first node of the oscillation $r_{\text{node}}$ is shown along with the first induced density minimum, scaled by the average electron density, $\Delta\rho_{\min}/\rho_0$. The data are from the Green's-function method and from Perrot.

| | | This work | | Perrot | |
|---|---|---|---|---|---|
| $r_s$ | $t$ | $r_{\text{node}}$ | $\Delta\rho_{\min}/\rho_0$ | $r_{\text{node}}$ | $\Delta\rho_{\min}/\rho_0$ |
| 2.0 | 0.5 | 8.48 | $-1.25\times10^{-6}$ | 10.7 | $-8.7\times10^{-8}$ |
| 4.0 | 0.5 | 3.50 | $-7.55\times10^{-2}$ | 3.48 | $-7.8\times10^{-2}$ |
| 4.0 | 1.0 | 5.51 | $-2.00\times10^{-3}$ | 5.56 | $-5.4\times10^{-4}$ |

For each induced electron density, the value of $R_0$ is determined by Perrot such that the above relationship is satisfied. This in turn defines an inverse screening length value for that density.

The values calculated with the Green's-function method can be seen to be in good agreement with those calculated by Perrot. The agreement is stronger for the inverse screening length values than for the induced density values at the origin, which are systematically greater in the Green's-function calculation. The induced density at the origin does not make significant contributions to the total Coulomb potential of the electrons. Its exact value there is less important than the density values away from the origin.

At low temperatures, the electron density around the proton exhibits Friedel oscillations [24]. The effect is strongest at zero temperature where there is a sharp cutoff in allowed momentum at the Fermi energy, in which case a smooth density distribution cannot be formed. As the temperature is increased, the oscillations disappear. The parameters for which Friedel oscillations were found to exist can be seen in Table III. The oscillations were exhibited for the same parameters in both the Green's-function calculation and in Perrot's. The quantity $r_{\text{node}}$ is the first node in the induced density, i.e., the first point where the induced density is zero.

As shown in Table III, the positions of the first nodes are in good agreement for $r_s=4.0$. The induced density values at the first minimum $\Delta\rho_{\min}/\rho_0$ are also similar for $r_s=4.0$ and $t=0.5$. Note that the other two minimums occur further out in the tail, where the induced density is small relative to the average value. If the induced density at each minimum is compared to the induced density at the origin, their relative values are even smaller. Differences in the values calculated with the two methods in this region are not significant.

### B. A neon nucleus in an electron gas

The screening of a neon nucleus in an electron gas has also been studied by Perrot [25]. The larger charge of neon, $Z=10$, makes for more polarization and a more stringent test of the Green's-function method.

The induced electron density values at the origin are shown in Table IV along with two quantities $R_0$ and $R_1$, which measure the charge distribution around the nucleus. The first set of numbers are those calculated with the Green's-function method, and the second set was calculated by Perrot. The quantity $R_0$ was defined in Eq. (47) as the radius of a sphere containing charge $0.549Z$. For the neon calculation, Perrot defined a new variable $R_1$, which is the radius where the induced density is equal to half the average density, $\Delta\rho(R_1)=\rho_0/2$.

TABLE IV. The induced electron density at the neon nucleus $\Delta\rho(0)$ and the variables $R_0$, $R_1$ for an electron gas with Wigner-Seitz radius $r_s=2.0$, calculated using the Green's-function method and the same quantities for the standard density functional calculation due to Perrot.

| | This work | | | Perrot | | |
|---|---|---|---|---|---|---|
| $t$ | $\Delta\rho(0)$ | $R_0$ | $R_1$ | $\Delta\rho(0)$ | $R_0$ | $R_1$ |
| 0.5 | | | | 591.6 | 0.835 | 1.891 |
| 1.0 | 557.7 | 0.868 | 2.133 | 592.3 | 0.867 | 2.069 |
| 2.0 | 496.1 | 1.004 | 2.264 | 590.9 | 1.003 | 2.259 |
| 4.0 | 489.4 | 1.879 | 2.335 | 468.2 | 1.842 | 2.362 |

As with the results for the screening of a proton, the variables describing the extent of the charge are in better agreement than the induced density values at the origin. The agreement of the charge distribution results improves as the temperature is raised.

### C. The method has no problems with bound states or high temperatures

In a Kohn-Sham wave function type calculation, the radial components of the single-particle eigenfunctions are found as solutions of the single-particle Schrödinger equation, Eq. (2). In the case of nuclei with large atomic numbers, there are many bound states to be found. In addition, for all nuclei there are shallow bound states at high temperatures and low densities.

The first difficulty presented by bound states is that they must be found. Since many of the eigenvalues can have small occupation factors, determining them can be difficult. A second problem posed by bound states stems from the fact that the density must be iterated until a self-consistent solution is found. In Perrot's neon calculation, for example, bound states were found to pop in and out of the continuum as the effective potential varied.

Bound states pose no such problem in the Green's-function method. The single-particle Green's function defined in Eq. (7) contains bound and continuum wave functions by construction. Thus, the bound states are included automatically with every iteration, and they do not need to be found separately before they can be included in the result for the density.

An interesting question to ask with regards to the iteration of the density and the Green's-function method is if the hopping of loosely bound states in and out of the continuum can lead to the same numerical problems described by Perrot. The answer has been given by Kohn and Majumdar [26], who showed that the properties of a Fermi gas, such as the density, are smooth or analytic for just such a transition of a state from bound to unbound. The instabilities in Perrot's calculation might therefore be attributed to the difficulties of locating all of the bound states for each iteration.

Not only are bound states handled easily with the Green's-function method, but high temperatures are also not a problem. In a standard Kohn-Sham calculation, the expression for the density includes an integral over continuum

wave functions. In order to evaluate the density at higher temperatures, the number of wave vectors for which the continuum wave functions must be calculated increases. Furthermore, the calculation of the wave functions becomes more difficult as the wave functions become more oscillatory. Thus, for a traditional wave function type calculation, higher temperatures equate to more work, which puts practical limits on the temperature range where the method can be used.

For the Green's-function method, on the other hand, higher temperatures present no such obstacles. Larger temperatures mean a greater distance between Matsubara poles, Eq. (10), which makes for faster convergence of the sum over these poles in Eq. (33). In addition, the Green's-function method avoids the difficulties of rapidly oscillating solutions by the use of logarithmic derivatives of the radial solutions, Eq. (28). The larger the complex wave number $\kappa$, the more well behaved the logarithmic derivatives become, Eqs. (30) and (31).

## VI. SUMMARY AND CONCLUSIONS

The screening of nuclei by electrons in a finite temperature plasma is considered using the Kohn-Sham formulation of density functional theory, with a local density term to describe exchange and correlation.

Rather than calculating single-particle wave functions, the problem is developed in terms of Green's functions which are evaluated at Matsubara poles lying along a line parallel to the imaginary axis. A finite number of poles is evaluated and the infinite sum required for the calculation of electron densities is effected by extrapolation and interpolation. Bound states are automatically included, which eliminates the numerical instabilities in wave function methods.

For complex energies close to the real axis, the inner and outer factors of the Green's function are obtained by direct integration. For energies far from the real axis, logarithmic derivatives of the factors are calculated, which is all that is required for the evaluation of the density. These logarithmic derivatives satisfy first-order differential equations and are smooth functions which actually become better behaved as the complex energy increases in magnitude. This obviates the problem of rapidly oscillating functions in the wave function formulation. The method is applicable to all temperatures, and converges especially well at high temperatures.

Numerical results are presented for protons and neon nuclei. Comparisons to earlier works by Perrot using a wave function formulation are given.

An important application of the method is evaluation of the effect of shielding on thermonuclear fusion rates in laboratory and stellar plasmas. A paper [27] is in preparation giving results for the solar core; it also incorporates the effect of shielding by the other positive nuclear constituents in the plasma.

## ACKNOWLEDGMENTS

One of us (L.W.) wishes to acknowledge a discussion with J. S. Cohen, LANL, which stimulated interest in the problem. The work was supported by a U.S. DOE grant.

[1] W. Kohn and L. J. Sham, Phys. Rev. **140**, A1133 (1965).
[2] R. M. Dreizler and E. K. U. Gross, *Density Functional Theory: An Approach to the Quantum Many-Body Problem* (Springer-Verlag, Berlin, 1990).
[3] R. G. Parr and W. Yang, *Density Functional Theory of Atoms and Molecules* (Oxford University Press, New York, 1989).
[4] D. R. Hartree, Proc. Cambridge Philos. Soc. **24**, 111 (1928).
[5] A. A. Katsnelson, V. S. Stepanyuk, A. I. Szász, and O. V. Farberovich, *Computational Methods in Condensed Matter: Electronic Structure* (AIP, New York, 1992).
[6] R. Zeller, P. Lang, B. Drittler, and P. H. Dederichs, in *Application of Multiple Scattering Theory to Materials Science*, edited by W. H. Butler, P. H. Dederichs, A. Gonis, and R. L. Weaver, MRS Symposia Proceedings No. 253 (Materials Research Society, Pittsburgh, 1992), p. 357.
[7] P. Lang, V. S. Stepanyuk, K. Wildberger, R. Zeller, and P. H. Dederichs, Solid State Commun. **92**, 755 (1994).
[8] K. Wildberger, P. Lang, R. Zeller, and P. H. Dederichs, Phys. Rev. B **52**, 11 502 (1995).
[9] N. W. Ashcroft and N. D. Mermin, *Solid State Physics* (Holt, Rinehart, and Winston, Orlando, 1976), p. 760.
[10] N. D. Mermin, Phys. Rev. **137**, A144 (1965).
[11] I. J. Thompson and A. R. Barnett, J. Comput. Phys. **64**, 490 (1986).
[12] M. Abramowitz, in *Handbook of Mathematical Functions*, edited by M. Abramowitz and I. A. Stegun (U.S. GPO, Washington, DC, 1964).
[13] H. A. Antosiewicz, in *Handbook of Mathematical Functions* (Ref. [12]).
[14] I. J. Thompson and A. R. Barnett, Comput. Phys. Commun. **36**, 363 (1985).
[15] I. J. Thompson and A. R. Barnett, computer code WCLBES, CERN Program Library, 1988.
[16] M. Golomb and M. Shanks, *Elements of Ordinary Differential Equations* (McGraw-Hill, New York, 1965), p. 332.
[17] G. Arfken, *Mathematical Methods for Physicists* (Academic Press, New York, 1985), p. 912.
[18] E. Merzbacher, *Quantum Mechanics* (John Wiley and Sons, New York, 1970).
[19] W. Kohn and L. J. Sham, Phys. Rev. **137**, A1697 (1965).
[20] G. Dahlquist and A. Björck, *Numerical Methods* (Prentice-Hall, Englewood Cliffs, NJ, 1974).
[21] M. J. Watrous, Ph.D. dissertation, University of Washington, Seattle, 1997.
[22] F. Perrot, Phys. Rev. A **25**, 489 (1982).
[23] F. Perrot and M. W. C. Dharma-wardana, Phys. Rev. A **30**, 2619 (1984).
[24] J. Friedel, Philos. Mag. **43**, 153 (1952).
[25] F. Perrot, Phys. Rev. A **26**, 1035 (1982).
[26] W. Kohn and C. Majumdar, Phys. Rev. **138**, A1617 (1965).
[27] L. Wilets, B. Giraud, M. J. Watrous, and J. J. Rehr, University of Washington Report No. NT@UW-98-6, 1998.